LA-UR-16-22099
Approved for public release; distribution is unlimited.

Title: Radiation Re-solution Calculation in Uranium-Silicide Fuels

Author(s): Matthews, Christopher
Andersson, Anders David Ragnar
Unal, Cetin

Intended for: Report

Issued: 2017-01-27 (rev.1)

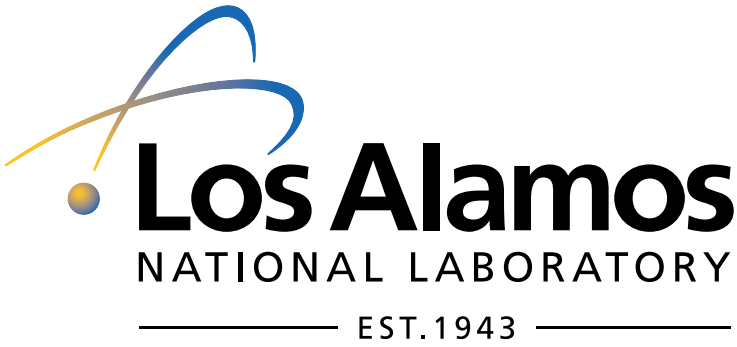

Radiation Re-solution Calculation in Uranium-Silicide Fuels

Christopher Matthews
David Andersson
Cetin Unal

March 2016

Contents

1 Introduction

The release of fission gas from nuclear fuels is of primary concern for safe operation of nuclear power plants. Although the production of fission gas atoms can be easily calculated from the fission rate in the fuel and the average yield of fission gas, the actual diffusion, behavior, and ultimate escape of fission gas from nuclear fuel depends on many other variables.

As fission gas diffuses through the fuel grain, it tends to collect into intra-granular bubbles, as portrayed in Figure 1.1. These bubbles continue to grow due to absorption of single gas atoms. Simultaneously, passing fission fragments can cause collisions in the bubble that result in gas atoms being knocked back into the grain. This so called "re-solution" event results in a transient equilibrium of single gas atoms within the grain. As single gas atoms progress through the grain, they will eventually collect along grain boundaries, creating inter-granular bubbles. As the inter-granular bubbles grow over time, they will interconnect with other grain-face bubbles until a pathway is created to the outside of the fuel surface, at which point the highly pressurized inter-granular bubbles will expel their contents into the fuel plenum. This last process is the primary cause of fission gas release.

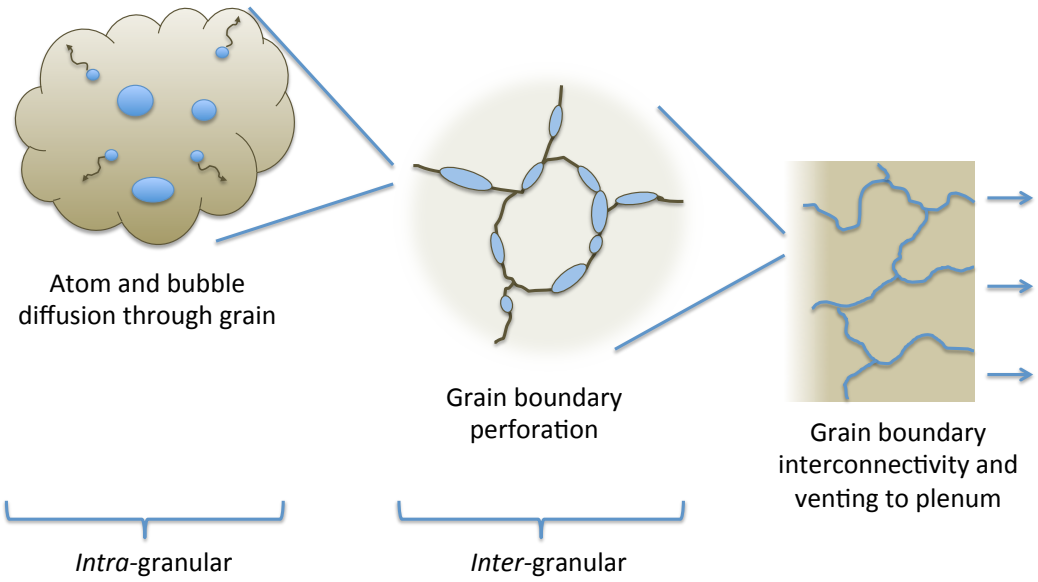

Figure 1.1: Schematic of fission gas behavior.

From the simple description above, it is clear there are several parameters that ultimately affect fission gas release, including the diffusivity of single gas atoms, the absorption and knockout rate of single gas atoms in intra-granular bubbles, and the growth and interlinkage of inter-

granular bubbles. Of these, the knockout, or re-solution rate has an particularly important role in determining the transient concentration of single gas atoms in the grain. The re-solution rate will be explored in the following sections with regards to uranium-silicide fuels in order to support future models of fission gas bubble behavior

2 Background

The total re-solution rate at which atoms are knocked back into the fuel can be calculated by,

$$R\left[\text{atom}/(\text{s}\cdot\text{m}^3)\right] = \int \dot{F} b(r) m(r) \rho(r) dr, \tag{2.1}$$

where r is the bubble radius, $\dot{F}$ is the fission rate, b is the re-solution parameter, m is the number of atoms in a bubble, and ρ is the bubble concentration distribution function,

$$N\left[\text{bub}/\text{m}^3\right] = \int \rho(r) dr. \tag{2.2}$$

Here, N is the total concentration of bubbles in the sample.

Using Equation 2.1, the physics of re-solution can be distilled in a single re-solution parameter for a given fuel type, b, effectively separating environmental variables such as fission rate, temperature, and the bubble concentration distribution. The re-solution parameter has units of knocked-out atoms per atoms in the bubble per fission, and essentially gives the probability of any given atom in a bubble to be knocked-out per fission.

The first conceptual model of fission gas re-solution was the so called homogeneous model presented by Nelson in 1969 [1]. The homogeneous model treats the collision of fission fragments ballistically, with gas atoms being knocked out of a gas bubble due to a collision with the fission fragments, or indirectly through a damage cascade produced by an adjacent fuel atom. Using the simplified Rutherford and hard-sphere potentials, Nelson was able to calculate a first estimate for re-solution rate in UO_2. Nelson's theory has primarily seen success in non-oxide fuels in which the bubbles grow to very large sizes, on the order of 100's of nanometers [2], but ultimately fails to capture the empirically estimated re-solution rate in UO_2.

In contrast to the chipping out process described by Nelson, Turbull's model of re-solution published in 1971 was based on the assumption of total-destruction of the fission gas bubble by passing fission fragments [3]. Relying on experimental evidence, Turbull claimed that if the path of the fission fragment traveled sufficiently close to a fission gas bubble (around 0.5 nm), the entire bubble would be destroyed and its contents of fission gas would be returned to the grain as single gas atoms. While this theory seemed applicable to UO_2 fuels in which the intra-granular bubbles remained small (on the order of 5 nm), it remained inapplicable to the large bubbles prevalent in other types of nuclear fuels.

The apparent conflict between the two re-solution theories lies directly with the difference of oxide nuclear fuel; calculations by Blank and Matzke showed that the poor thermal conductivity of UO_2 results in a very large, localized thermal spike around the passing fission fragment, on the order of 2000 K [4]. The large temperature gradient results in a strong thermo-mechanical pulse, causing mixing of the lattice and destruction of nearby bubbles [2]. The same calculations performed for uranium carbide, which benefits from a metallic-like thermal properties [4]

showed a corresponding thermal spike on the order of 50 K, with effectively no resulting thermo-mechanical pulse. In light of the differences between UO_2 and UC, it is easy to see why Turnbull's theory has seen success in oxide fuels, while Nelson's theory has seen success in non-oxide fuels [5].

Modern calculations of re-solution have focused on UO_2 through utilization of Molecular Dynamics (MD) simulations [6–8], but ultimately suffer from the high computational cost of MD. In light of the above discussion, re-solution in fuels with good thermal behavior can be modeled using the homogeneous model, allowing less computationally expensive models and codes to capture the re-solution behavior. Recently, the Binary Collision Approximation (BCA) has been utilized to calculate the re-solution rate in uranium carbide fuels for a wide range of bubble sizes [5]. Benefiting from the simplification of the collision kinematics to a two-body problem, the code 3DOT [5] utilizes the TRIM algorithm [9] to capture the full cascade behavior of fission fragments interacting with fission fragments in fuel. By leveraging modern methods and models, the 3DOT simulations calculated a re-solution parameter an order of magnitude lower than previous calculations due to the inclusion of electronic energy losses. In addition, the importance of secondary cascades (or cascades created in the fuel by passing fission fragments, resulting in a knockout of gas by a uranium atom) played a much bigger role in re-solution than direct collisions with fission fragments.

The applicability of the homogeneous re-solution theory lies in the mechanism with which fission fragments dissipate energy as they travel through the fuel. In the purely ceramic matrix of UO_2, the fission fragment relies on electron-phonon interactions or lattice vibrations to dissipate energy, while the metallic bonding in UC allows energy to be transferred primarily through the much more efficient electron-electron interaction. This behavior manifests itself in bulk thermal properties as well, namely thermal conductivity. From Figure 2.1, it is clear that the thermal conductivity of UO_2 is much less than all other fuels at temperatures of interest ($T>1000$ K). In the absence of a thorough understanding of all fuel types, thermal conductivity can be utilized as a first approximation of the applicability of homogeneous re-solution, allowing the 3DOT simulations to be extended to other fuel types following the same methodology presented in [5].

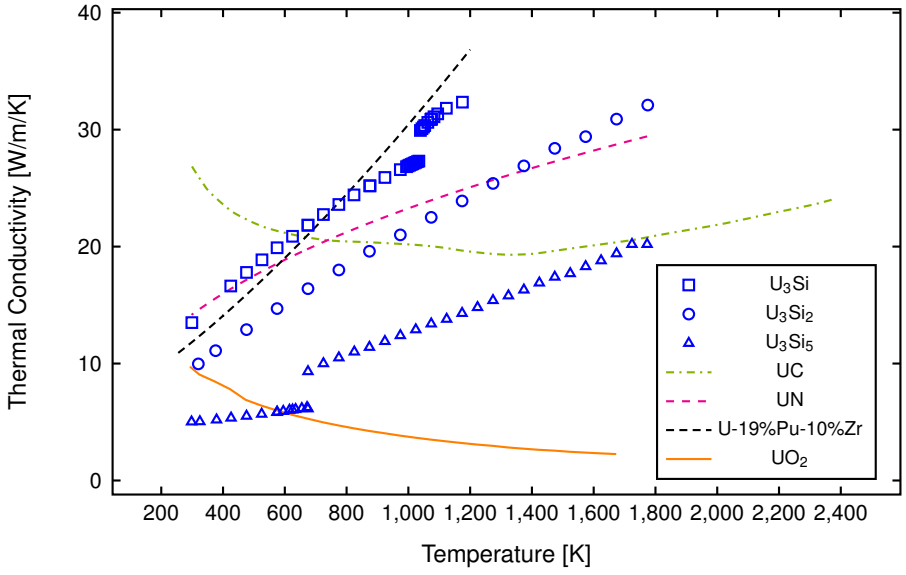

Figure 2.1: Thermal conductivities for U_3Si [10], U_3Si_2 [11], U_3Si_5 [12], UC [13], UN [14], U-19%Pu-10%Zr [15], and UO_2 [16].

3 Re-solution parameter Calculation

3.1 Methods

The code 3DOT was used to calculate the re-solution parameter for various non-oxide fuels, with parametric studies focused on U_3Si_2. 3DOT relies on BCA to reduce the collision kinematics to sequential two-body collisions by utilizing the previously published TRIM algorithm [9]. Full ion cascades are tracked from the creation of fission fragments until all ions fall below an energetic threshold. Electronic stopping power is calculated by scaling proton stopping powers using the Brandt-Kitagawa theory [9, 17]. Due to the nature of TRIM calculations, each ion interacts with an undamaged, 0 K amorphous target.

Each 3DOT simulation model consisted of a fuel cube with an implanted sphere of xenon, representing an intra-granular bubble. Since each simulation takes place entirely within the interior of the grain, theoretical densities are utilized and no grain-boundary effects are simulated. Owing to the small computation expense of BCA and the wide spread of bubble sizes present in non-oxide fuels [18], the simulated bubble radii ranged from 0.5 nm to 500 nm with periodic boundary conditions enforced on all box sides.

Considering the many combinations of bubble radii and box sizes, any dependence on simulation volume must be removed. Due to the periodic boundary conditions, the approximately 6 μm fission fragment path will wrap around the model many times. Due to the relatively low density within the bubble, as the porosity increases, the total fission fragment path will also increase. In order to avoid a bubble concentration dependent path length, comparative studies of various bubble and box sizes showed that the artificial lengthening of the fission fragment path was minimized when the cube length was at least 10 times the bubble radius. In this way, a value for b can be calculated independent of the bubble concentration.

For these calculations, a fission gas atom was considered implanted if it exited the bubble surface with an implantation energy greater than E_{min}. The value of E_{min} = 300 eV first utilized by Nelson has been implemented in many re-solution studies [1, 2, 7]. More recently, a study aimed at determining the implantation energy in UO_2 fuels determined that while re-solution did occur for atoms with implantation energies less than the 300 eV, the original implantation energy of 300 eV resulted in a 85% probability of re-solution [19]. In light of this, the value of E_{min} = 300 eV will be utilized unless otherwise specified, although model sensitivity to this value will be explored.

In stress free solids, the number of atoms in a bubble m is generally calculated using the Van der Waals equation of state (EOS):

$$m = \frac{4}{3}\pi r^3 (B + kTr/2\gamma)^{-1} \tag{3.1}$$

where γ is the surface energy, k is Boltmann's constant, T is temperature, and $B = 8.5 \cdot 10^{-29}$

m^3/atom [20]. In reality, the high temperature and stress involved with very small bubbles in nuclear fuel results in an underestimation of atomic density [21, 22]. However, due to the lack of a more sophisticated EOS for uranium silicides, Equation 3.1 will be utilized with a nominal surface energy of $\gamma = 1$ N/m until better data is available. Sensitivity to γ and T will be explored as well.

Table 3.1 lists the relevant simulation parameters for the 3DOT simulations.

Table 3.1: Simulation Parameters

Parameter	Value
U_3Si Density [23]	15.4 g/cm^3
U_3Si_2 Density [24]	12.2 g/cm^3
U_3Si_5 Density [12]	9.06 g/cm^3
UC Density [25]	13.6 g/cm^3
UN Density [25]	14.3 g/cm^3
U-19%Pu-10%Zr Density	15.8 g/cm^3
Nominal Surface tension, γ	1.0 N/m
Nominal Temperature, T	1000 K
E_{min}	300 eV

The parameter of interest in each 3DOT simulations is the total number of gas atoms knocked out of the bubble. Since the simulations are essentially random, the error in the escaped atom per fission tally can be estimated by the square-root of total number of fissions F_{tot}. For the simulations that follow, the criteria,

$$1/\sqrt{F_{tot}} \leq 0.001, \tag{3.2}$$

was utilized, requiring a range of fission evets from $7{\cdot}10^4$ for the smallest bubbles, to $7{\cdot}10^6$ for the largest bubble size. By following the criteria in Equation 3.2, comparisons between separate but identical simulations with the same number of accumulated fission events results in less than a 1% deviation in b.

3.2 Results

The re-solution parameter for several fuel types is displayed in Figure 3.2. In general, the higher the uranium content, the higher the re-solution parameter. In the previous 3DOT study, it was shown that the primary cause of re-solution of gas atoms is due to knocked uranium atoms entering the bubble [5]. By increasing the heavy metal atom fraction, more uranium atoms are struck by fission fragments, resulting in an increase of the re-solution parameter. This effect results in an increased re-solution parameter for silicide fuels with less Si content.

The heavy metal density can be modified both through density (i.e. theoretical density in uranium-silicide fuels increases as the silicon content increases), and through increasing the uranium atom ratio. This second cause can be isolated by calculating the re-solution parameter

for the uranium-silicide fuels at an artificial constant density. As seen in Figure 3.3, the re-solution parameter is largest for U_3Si, with a heavy metal atom ratio of 3:1, and lowest for U_3Si_5 with heavy metal ratio of 3:5.

All simulations presented here assume the uranium content consists of only uranium-238. In actuality, nuclear fuels will likely be enriched in uranium-235, changing the average mass of uranium in the simulation. The re-solution parameter for U_3Si_2 using 50% uranium-235 is overlaid the nominal re-solution parameter calculated for U_3Si_2 in Figure 3.2. With such a small decrease in mass (average of 236.5 instead of 238), almost no change in re-solution parameter is evident. As such, the assumption of 100% uranium-238 is maintained throughout the remainder of the simulations.

One of the biggest parameters that determines the re-solution parameter is the density of gas within the bubble. For bubbles with high fission gas density, the collision probability increases, but a struck fission gas atom must take a more tortuous path to escape the bubble. Conversely, for low fission gas densities, the probability of an atom being stuck decreases, but the mean free path of a traveling fission gas atom increases. Since the two unknowns in Equation 3.1 are temperature and surface tension, the factor T/γ is a convenient parameter to describe the EOS at various values, as displayed in Figure 3.5. As temperature increases or the surface tension decreases, the atomic density in the bubble decreases. This in turn increases the re-solution parameter, as displayed in Figures 3.6 and 3.7. Conversely, decreasing the temperature or increasing the surface tension results in an overall decrease in the re-solution parameter.

In general, the shape of intra-granular bubbles will be spherical in order to minimize the system energy. In contrast, grain-face bubbles will maintain a lenticular shape due to the bubble location squeezing between grain boundaries. By modifying the shape of the bubble in 3DOT simulations, insight can be gained into how the bubble shape will modify the re-solution rate. In general, an ellipsoid can be described by the half-lengths of its three axis, a, b, and c. Assuming that two out of three axis are identical $a = b$, the ratio of third axis can be described using a shape parameter, $S = c/a$, where $S = 1$ describes a sphere in which $R = a = b = c$. Unfortunately, the van der Waals equation of state is built for bubbles in equilibrium with the bulk, which explicitly does not describe ellipsoid bubbles, therefore it is assumed that spheres and ellipsoid bubbles with the same volume contain the same number of gas atoms. Following this assumption, the axis of the ellipsoid can be determined by,

$$a = b = RS^{-1/3}, \tag{3.3a}$$

$$c = Sa. \tag{3.3b}$$

Examples of the ellipsoid shapes for a given shape factor is displayed in Figure 3.1. 3DOT simulations of various values of S are displayed in Figure 3.8. As the shape parameter decreases, the fraction of gas atoms neighboring the fuel increases. As discussed in the previous study, traveling uranium atoms are the root cause for re-solution [5]. As the fraction of gas atoms at risk for collision with a uranium atom increases, the re-solution parameter also increases. This is especially prevalent in large ellipsoid bubbles with very small shape factors.

The effect of bubble concentration on b can be simulated by changing the 3DOT simulation box size, as displayed in Figure 3.9. The re-solution parameter increases as a function of concentration due to an increase in the total fission fragment flight path as the average density of

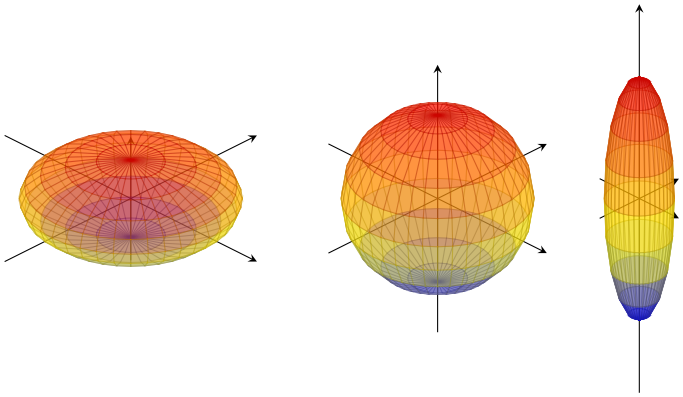

Figure 3.1: Ellipsoids with shape factors of 0.4, 1.0, and 4.0.

the total simulation space decreases. However, the total increase is minimal when compared to other factors such as temperature. Figure 3.9 also provides verification of the assumption utilized in the other simulations that a box size of 10 times the bubble radius provides a calculation independent of bubble concentration.

It should be noted that the re-solution parameter describes the knockout probability of a gas atom within the bubble as described in Section 2, not explicitly the re-solution rate. In order to calculate the re-solution rate, Equation 2.1 must be utilized. Combining the re-solution parameter with the total number atoms in a bubble gives some insight into the total re-solution rate. From Table 3.2 and Figure 3.10 it is clear that variations in temperature will modify the re-solution parameter, however the overall variation in the re-solution parameter is minuscule compared to the vast order of magnitude differences in the product $b * m$.

Lastly, one of the important parameters utilized to calculate the re-solution parameter is the threshold implantation energy, E_{min}. The calculated re-solution parameter using different values of E_{min} is displayed in Figure 3.11. As expected, the re-solution parameter increases as E_{min} decreases, yet the deviations are still minor when compared to the values of $b * m$ plotted in Figure 3.10. As such, the value of $E_{min} = 300$ eV remains a valid assumption until more robust data can be obtained.

Table 3.2: Values of $b * m$ for various temperatures

Bubble Radius [nm]	$T = 500$ K	$T = 750$ K	$T = 1000$ K	$T = 1250$ K	$T = 1500$ K
0.5	1.75E-24	1.74E-24	1.71E-24	1.71E-24	1.69E-24
5	7.68E-22	7.53E-22	7.19E-22	6.99E-22	6.73E-22
50	1.11E-19	1.08E-19	1.01E-19	9.67E-20	9.30E-20
500	1.18E-17	1.12E-17	1.05E-17	1.01E-17	9.53E-18

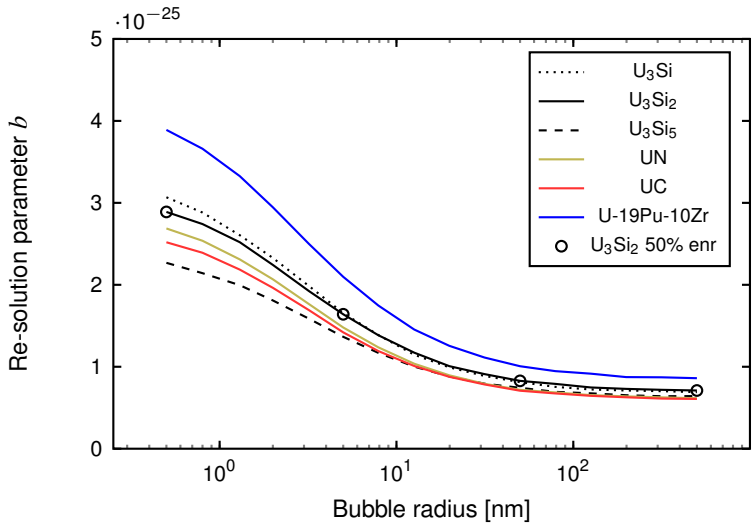

Figure 3.2: Re-solution parameter calculation for several fuel types using the values in Table 3.1.

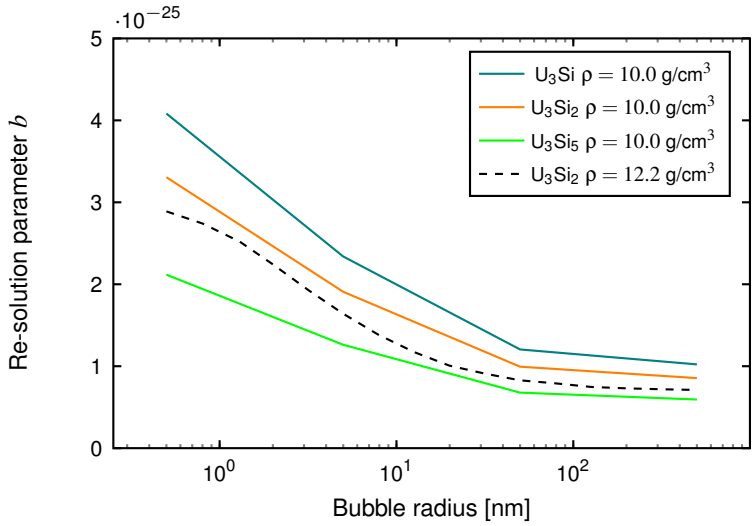

Figure 3.3: Re-solution parameter calculation for different silicide fuels with the exact same density of 10 g/cm^3.

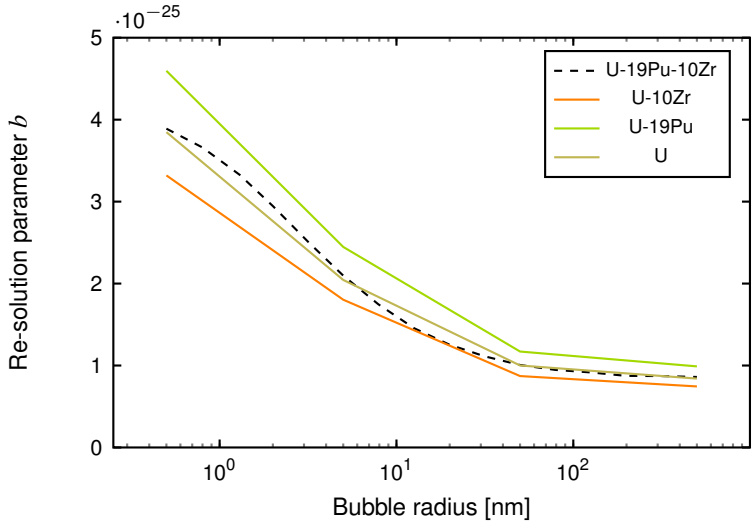

Figure 3.4: Re-solution parameter calculation for different atom concentrations in U-Pu-Zr fuels.

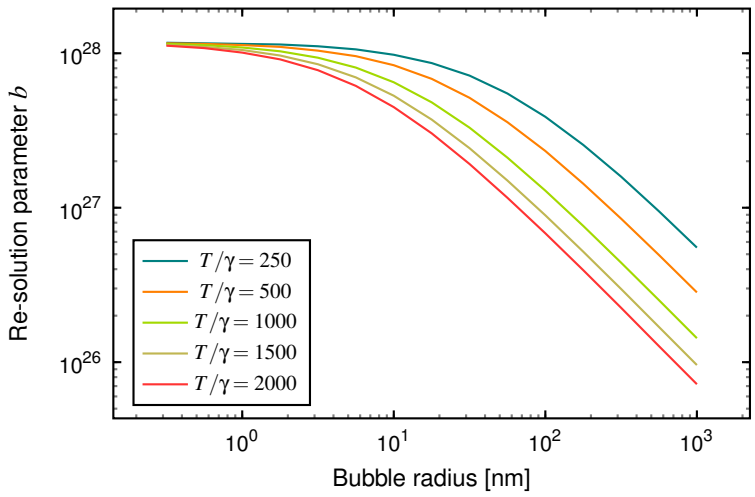

Figure 3.5: Atomic density in the bubble using several different parameters for the Van der Waal's equation of state described in Equation 3.1.

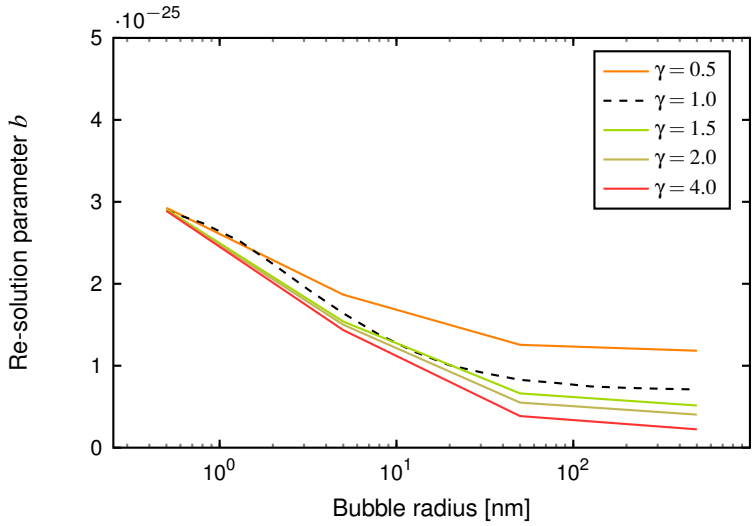

Figure 3.6: Re-solution parameter calculation for several values of γ in U_3Si_2.

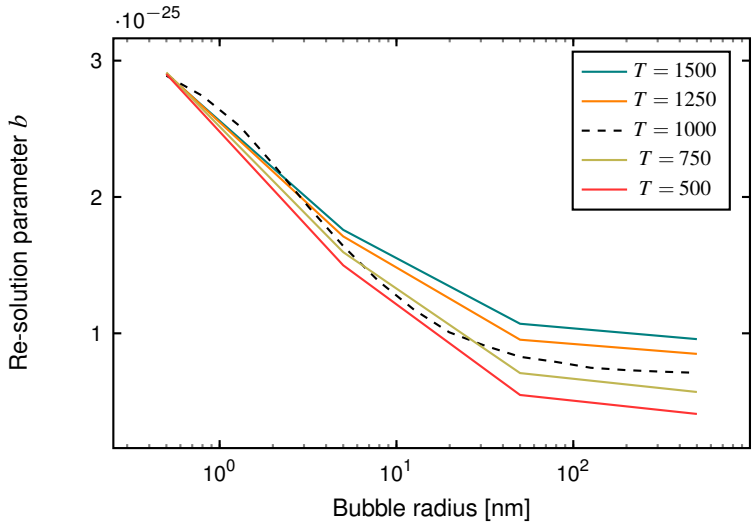

Figure 3.7: Re-solution parameter calculation for several values of T in U_3Si_2.

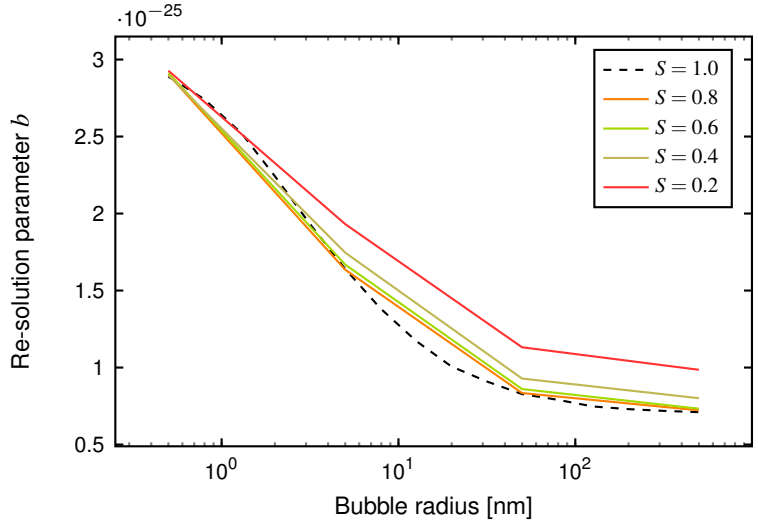

Figure 3.8: Re-solution parameter calculation for several values of the shape parameter S in U_3Si_2.

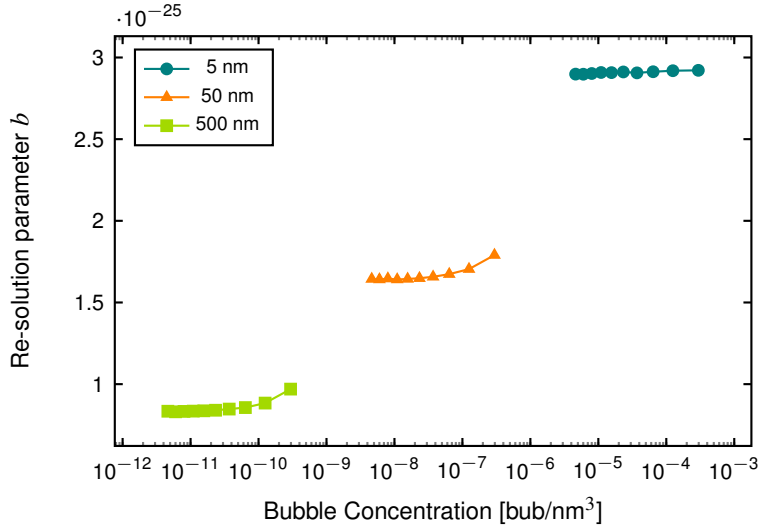

Figure 3.9: Re-solution parameter calculation as a function of bubble concentration in U_3Si_2.

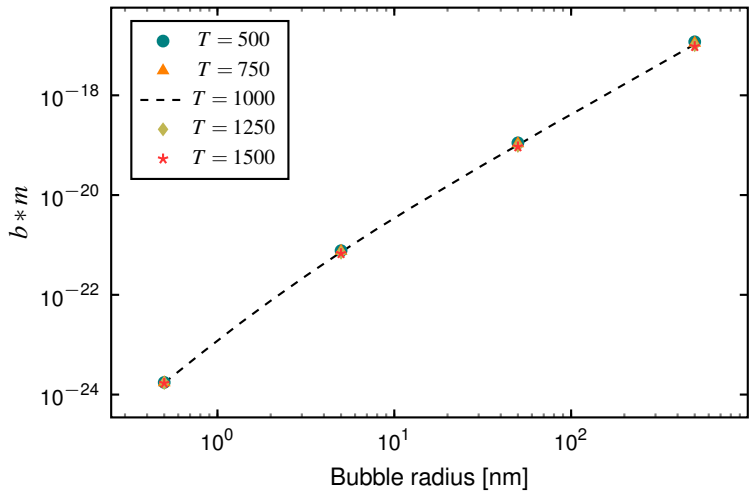

Figure 3.10: $b * m$ calculation for several values of T, along with the parameters included in Table 3.1.

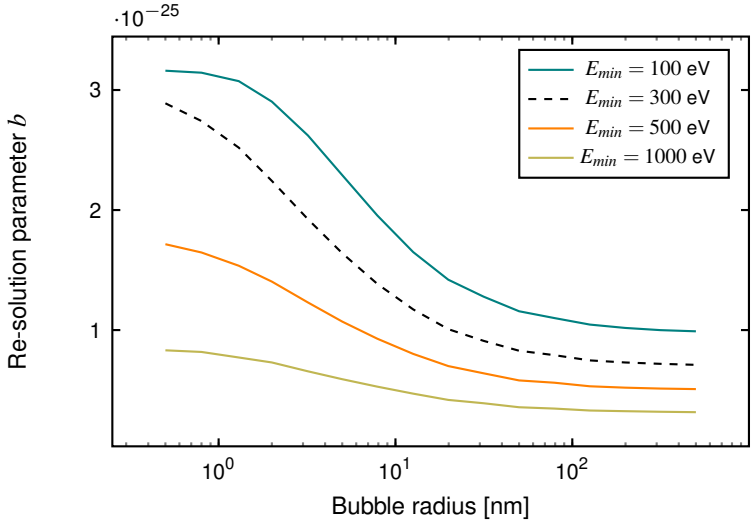

Figure 3.11: Re-solution parameter calculation for several values of E_{min} in U_3Si_2.

4 Conclusions

Using the BCA code 3DOT, the re-solution parameter was calculated for a variety of non-oxide fuels, with parametric studies on several important parameters explored for U_3Si_2 fuels. In general, the heavy metal density of the fuel determines the re-solution parameter, with higher fractions resulting in more gas atom collisions and a higher re-solution parameter. This is dependent on both the heavy metal atom ratio, and the theoretical density of the fuel.

Although values for the surface energy are absent for uranium-silicide fuels, a parametric study in U_3Si_2 fuels showed that varying γ from 0.5 to 4 N/m primarily impacted the re-solution parameter for very large bubbles, with larger values of γ resulting in a smaller re-solution parameter. Similar deviations were achieved by changing the temperature from 500 to 1500 K, in which higher temperatures results in higher re-solution parameters. Both γ and T modify the atomic density of fission gas within the bubble, with smaller densities allowing struck atoms to more easily reach the bubble surface, and increasing the re-solution parameter.

Changing the shape of the bubble to an ellipsoid also increased re-solution parameter due a higher fraction of gas atoms neighboring the fuel. This results in a larger fraction of struck fuel atoms entering the bubble, which was previously determined to be the primary cause of re-solution [5].

The largest deviation in the re-solution parameter is a result of the threshold implantation energy, with a deviation of nearly 30% over all bubble sizes as E_{min} is changed from 100 to 1000 eV.

When the differences in the re-solution parameter are compared to the product $b * m$, the slight variations become minor when compared to the order-of-magnitude increase in $b * m$ as the bubble sizes range from 0.5 nm to 500 nm.

References

[1] R. S. Nelson, The stability of gas bubbles in an irradiation environment, Journal of Nuclear Materials 31 (2) (1969) 153–161.

[2] C. Ronchi, P. T. Elton, Radiation re-solution of fission gas in uranium dioxide and carbide, Journal of Nuclear Materials 140 (3) (1986) 228–244.

[3] J. A. Turnbull, The distribution of intragranular fission gas bubbles in UO_2 during irradiation, Journal of Nuclear Materials 38 (2) (1971) 203–212.

[4] H. Blank, Properties of fission spikes in UO2 and UC due to electronic stopping power, Physica Status Solidi (a) 10 (2) (1972) 465–478.

[5] C. Matthews, D. Schwen, A. C. Klein, Radiation re-solution of fission gas in non-oxide nuclear fuel, Journal of Nuclear Materials 457 (C) (2015) 273–278.

[6] D. C. Parfitt, R. W. Grimes, Predicted mechanisms for radiation enhanced helium resolution in uranium dioxide, Journal of Nuclear Materials 381 (3) (2008) 216–222.

[7] D. Schwen, M. Huang, P. Bellon, R. S. Averback, Molecular dynamics simulation of intragranular Xe bubble re-solution in UO_2, Journal of Nuclear Materials 392 (1) (2009) 35–39.

[8] K. Govers, C. L. Bishop, D. C. Parfitt, S. E. Lemehov, M. Verwerft, R. W. Grimes, Molecular dynamics study of Xe bubble re-solution in UO_2, Journal of Nuclear Materials 420 (1-3) (2012) 282–290.

[9] J. F. Ziegler, J. P. Biersack, The Stopping and Range of Ions in Matter, in: Treatise on Heavy-Ion Science, Springer US, Boston, MA, 1985, pp. 93–129.

[10] J. T. White, A. T. Nelson, D. D. Byler, J. A. Valdez, K. J. McClellan, Thermophysical properties of U_3Si to 1150K, Journal of Nuclear Materials 452 (1-3) (2014) 304–310.

[11] H. Shimizu, The Properties and Irradiation Behavior of U3Si2, Tech. Rep. NAA-SR-10621 (1965).

[12] J. T. White, A. T. Nelson, D. D. Byler, D. J. Safarik, J. T. Dunwoody, K. J. McClellan, Thermophysical properties of U_3Si_5 to 1773K, Journal of Nuclear Materials 456 (C) (2015) 442–448.

[13] E. K. Storms, An Analytical Rpresentation of the Thermal Conductivity and Electrical Resistivity of $UC_{1\pm x}$ PuC_{1-x} and $(U_yPu_{1-y})C_{1\pm x}$, Tech. Rep. LA-9524, Los Alamos National Laboratory (Dec. 1982).

[14] S. B. Ross, M. S. El-Genk, R. B. Matthews, Thermal conductivity correlation for uranium nitride fuel between 10 and 1923 K, Journal of Nuclear Materials 151 (3) (1988) 318–326.

[15] J. Galloway, C. Unal, N. Carlson, D. Porter, S. Hayes, Modeling constituent redistribution in U–Pu–Zr metallic fuel using the advanced fuel performance code BISON, Nuclear Engineering and Design 286 (2015) 1–17.

[16] J. T. White, A. T. Nelson, Thermal conductivity of UO_{2+x} and U_4O_9, Journal of Nuclear Materials 443 (1-3) (2013) 342–350.

[17] W. Brandt, M. Kitagawa, Effective stopping-power charges of swift ions in condensed matter, Physical Review B 25 (9) (1982) 5631–5637.

[18] H. Blank, Nonoxide ceramic nuclear fuels, in: Nuclear materials, Vol 10a, 1994.

[19] D. C. Parfitt, R. W. Grimes, Predicting the probability for fission gas resolution into uranium dioxide, Journal of Nuclear Materials 392 (1) (2009) 28–34.

[20] D. R. Olander, Fundamental aspects of nuclear reactor fuel elements, Tech. rep., Technical Information Center, U.S. Department of Energy (Jan. 1976).

[21] C. Ronchi, Extrapolated equation of state for rare gases at high temperatures and densities, Journal of Nuclear Materials 96 (3) (1981) 314–328.

[22] K. Nogita, K. Une, High resolution TEM observation and density estimation of Xe bubbles in high burnup UO_2 fuels, Nuclear Instruments and Methods in Physics Research Section B: Beam Interactions with Materials and Atoms 141 (1-4) (1998) 481–486.

[23] V. P. Sinha, G. P. Mishra, S. Pal, K. B. Khan, P. V. Hegde, G. J. Prasad, Development of powder metallurgy technique for synthesis of U3Si2 dispersoid, Journal of Nuclear Materials 383 (1-2) (2008) 196–200.

[24] J. T. White, A. T. Nelson, J. T. Dunwoody, D. D. Byler, D. J. Safarik, K. J. McClellan, Thermophysical properties of U_3Si_2 to 1773K, Journal of Nuclear Materials 464 (C) (2015) 275–280.

[25] A. Zaoui, Continuum Micromechanics: Survey, Journal of Engineering Mechanics 128 (8) (2002) 808–816.